Available online at www.sciencedirect.com
SCIENCE DIRECT®
PERGAMON
International Journal of Heat and Mass Transfer 46 (2003) 1241–1249
International Journal of HEAT and MASS TRANSFER
www.elsevier.com/locate/ijhmt

Cooling enhancement in an air-cooled finned heat exchanger by thin water film evaporation

Chan Ho Song [a], Dae-Young Lee [b,*], Sung Tack Ro [a]

[a] School of Mechanical and Aerospace Engineering, Seoul National University, Seoul 151-742, Republic of Korea
[b] Thermal/Flow Control Research Center, Korea Institute of Science and Technology, Seoul 130-650, Republic of Korea

Received 18 January 2002; received in revised form 10 July 2002

Abstract

A theoretical analysis on the cooling enhancement by applying evaporative cooling to an air-cooled finned heat exchanger is presented in this work. A two-dimensional model on the heat and mass transfer in a finned channel is developed adopting a porous medium approach. Based on this model, the characteristics of the heat and mass transfer are investigated in a plate-fin heat exchanger with the interstitial surface fully covered by thin water film. Assuming that the Lewis number is unity and the water vapor saturation curve is linear, exact solutions to the energy and vapor concentration equations are obtained. The cooling effect with application of evaporative cooling was found to be improved considerably compared with that in the sensible cooler. This is because the thermal conductance between the fin and the air increases due to the latent heat transfer caused by the water evaporation from the fin surface. It is also found that the cooling enhancement depends greatly on the fin thickness. If the fin is not sufficiently thick, the cooling enhancement by the evaporative cooling decreases since the fin efficiency drops considerably due to the water evaporation from the fin surface. The fin thickness in the evaporative cooler should be increased larger than that in the sensible cooler to take full advantage of the cooling enhancement by the water evaporation.

Keywords: Evaporative cooling; Air-cooled finned heat exchanger; Cooling enhancement; Porous media; Water film; 2-D model

1. Introduction

Heat can be dissipated more effectively if the cooling effect brought by water evaporation is applied to a heat exchanger. Common examples of such application include cooling towers, evaporative condensers, evaporative coolers, etc. In such devices, heat from the hot fluid is dissipated to the atmospheric air by direct or indirect contact through not only sensible heat exchange but also evaporative latent heat exchange. The cooling performance is greatly improved by the effect of water evaporation [1–5].

Since heat and mass transfer occur simultaneously in an evaporative heat exchanger, the cooling process in an evaporative heat exchanger is more complex compared with that in a sensible heat exchanger. Maclaine-Cross and Banks [6] analyzed the evaporative heat transfer between parallel plates through a 1-D approach. They suggested a simplified analysis model assuming the Lewis number being unity and the water-vapor-saturation line being linear. With a similar approach, Kettleborough and Hsieh [7] showed that the wet bulb temperature is the most important factor to the performance of an evaporative heat exchanger. Hsu et al. [8] worked on the optimal design of an evaporative cooler based on a 1-D analysis. Chen et al. [9] proposed the performance evaluation method for the evaporative coolers in cylindrical or plate shapes. Recently, Stoitchkov and Dimitrov [10] studied the evaporative cooling in a cross-flow plate heat exchanger with a more improved Maclaine-Cross and Banks [6]' model. All the studies mentioned above were based on 1-D models. These models have to depend on the experimental data or

* Corresponding author. Tel.: +82-2-958-5674; fax: +82-2-958-5689.
E-mail address: ldy@kist.re.kr (D.-Y. Lee).

0017-9310/03/$ - see front matter © 2002 Elsevier Science Ltd. All rights reserved.
PII: S0017-9310(02)00405-2

Nomenclature

a	fin surface area per unit volume of the channel, 1/m
Bi	Biot number defined in Eq. (24)
c_p	specific heat of the air–water vapor mixture, J/(kg dry air K)
c_{wb}	specific heat of the saturated air, J/(kg dry air K)
F_l	fin length, m
F_p	fin pitch, m
F_t	fin thickness, m
g_{sat}	slope of the saturation curve in the psychrometric chart, kg/(kg dry air K)
h_D	interstitial mass transfer coefficient, kg dry air/(m^2 s)
h_i	interstitial heat transfer coefficient, W/(m^2 K)
h_w	wall heat transfer coefficient defined in Eq. (30), W/(m^2 K)
H	half height of the channel, m
i	enthalpy, J/(kg dry air)
i_{fg}	evaporative latent heat, J/(kg dry air)
j	Colburn j factor
k	thermal conductivity, W/(m K)
L_l	louver length, m
L_p	louver pitch, m
Le	Lewis number
Nu	Nusselt number
Pr	Prandtl number
q	heat flux, W/m^2
q_f	heat flux transferred from fin to air, W/m^2
q_{max}	maximum heat flux, W/m^2
Re	Reynolds number
St	Stanton number
T	temperature, K
T_d	tube depth, m
T_p	tube pitch, m
x, y	spatial coordinate, m
U	Darcian velocity of the air, m/s
v	interstitial air velocity, m/s

Greek symbols

ε	porosity
γ	mass diffusion coefficient, kg dry air/(m s)
η	nondimensional transverse coordinate defined in Eq. (17)
η_f	fin efficiency
θ	nondimensional temperature defined in Eq. (17)
Θ_L	louver angle, degree
κ	ratio of the effective conductivities between the air and the fin
λ	parameter defined in Eq. (27)
ρ	density, kg dry air/m^3
ω	humidity ratio, kg/kg dry air
Ω	nondimensional humidity defined in Eq. (17)
ζ	specific heat ratio defined in Eq. (11)

Subscripts

a	air
db	dry bulb
E	evaporative cooler
eff	effectiveness
f	fin
S	sensible cooler
wall	wall
wb	wet bulb
$\langle\ \rangle$	average over the channel cross-section

more sophisticated theoretical analysis regarding heat and mass transfer coefficients.

Meanwhile, Tsay [11] analyzed the heat and mass transfer in a plate channel covered with thin water film based on a 2-D model and evaluated the heat and mass transfer coefficients. He also showed that the latent heat transfer is more influential than the sensible heat transfer on the heat transfer performance. Yan [12,13] studied the evaporative cooling of a liquid film by turbulent mixed convection through a 2-D analysis and investigated the effect of the water supply temperature and mass flow rate.

Obviously, the 2-D analysis can provide more detailed information on the heat and mass transfer in evaporative coolers. Due to the complexity of the model, however, such 2-D analysis has been limited to very simple structures like plates. In general, practical heat exchangers are more complicated in shape because an extended surface is commonly added to enhance the heat transfer. Therefore, a more feasible 2-D model to analyze the heat and mass transfer and to evaluate the performance of evaporative cooling in such complicated configurations is needed.

The main purpose of this study is to investigate how much the cooling effect can be improved with the application of evaporative cooling in a conventional air-cooled heat exchanger. For instance, the cooling enhancement in a louvered fin heat exchanger as shown in Fig. 1 is considered when the interstitial surface of the heat exchanger is fully covered with thin water film. The heat exchanger is simplified as a channel filled with a porous medium and a 2-D model is developed to analyze

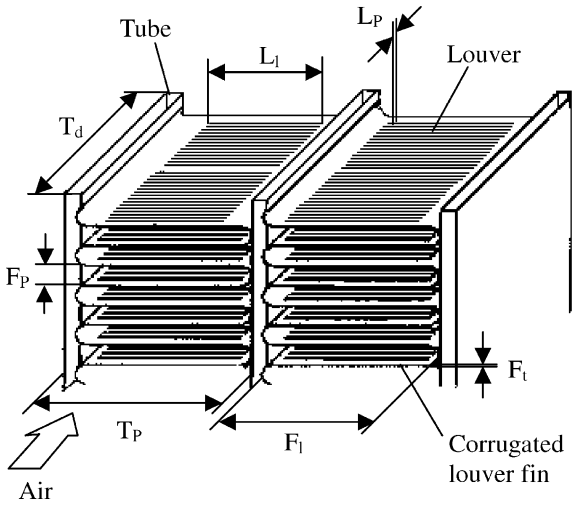

Fig. 1. A louvered fin heat exchanger.

the heat and mass transfer in the channel. Theoretical solutions to the temperature and moisture distributions are obtained and the cooling enhancement from the water evaporation is examined. In addition to this, the parameters dominating the heat and mass transfer characteristics are introduced and the fundamental mechanism of the cooling enhancement is investigated comprehensively.

2. Modeling

A schematic diagram of the problem presented in this study is shown in Fig. 2. The channel is filled with fins, whose surfaces are covered with thin water film. The height of the channel is $2H$, and a constant heat flux, q_{wall}, is applied to the channel wall. The heat and mass transfer around the fins and the channel wall are displayed more in detail also in the figure. The heat transferred to the water film either directly from the channel wall or via the fin is finally transferred into the air stream in forms of the sensible heat and the evaporative latent heat.

If the water film is negligibly thin, the thermal resistance across the water film is negligibly small. In such a case, the local temperature of the water film can be assumed the same as that of the solid surface adjacent to it. Besides this, the following assumptions are invoked.

- Flow and heat transfer in the channel are fully developed.
- Variation of thermophysical properties with temperature is negligible.
- Natural convection and radiation heat transfer are negligible.

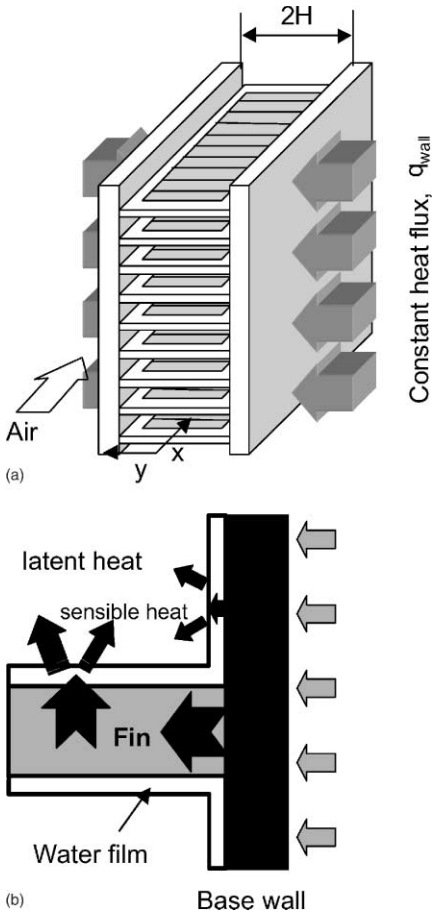

Fig. 2. A finned heat exchanger with thin water film on the interstitial surface: (a) schematic of the finned channel; (b) heat transfer process in the channel covered with thin water film.

- Water film is continuously replenished at its surface with water at the same temperature.

The heat transfer process in the channel as shown in Fig. 2 is known to be analyzed very exactly through the porous medium approach in which the fin and the air are separated and integrated locally to give two separate energy equations [14,15]. A similar approach is applied in this problem, and the resulting energy equations are obtained as follows:

Air stream

$$k_{a,eff}\frac{\partial^2 T_{a,db}}{\partial y^2}+\gamma_{eff}\frac{\partial^2 \omega_a}{\partial y^2}i_{fg}+h_i a(T_f-T_{a,db}) + h_D a(\omega_f-\omega_a)i_{fg}=\rho U\frac{\partial i_a}{\partial x} \quad (1)$$

Fin and water film

$$k_{\mathrm{f,eff}}\frac{\partial^2 T_{\mathrm{f}}}{\partial y^2} - h_{\mathrm{i}}a(T_{\mathrm{f}} - T_{\mathrm{a,db}}) - h_{\mathrm{D}}a(\omega_{\mathrm{f}} - \omega_{\mathrm{a}})i_{\mathrm{fg}} = 0 \tag{2}$$

For plate fin heat exchangers, the effective conductivities, $k_{\mathrm{a,eff}}$ and $k_{\mathrm{f,eff}}$, and the specific surface area, a, can be expressed as

$$k_{\mathrm{a,eff}} = \varepsilon k_{\mathrm{a}} = (1 - F_{\mathrm{t}}/F_{\mathrm{p}})k_{\mathrm{a}},$$
$$k_{\mathrm{f,eff}} = (1-\varepsilon)k_{\mathrm{f}} = (F_{\mathrm{t}}/F_{\mathrm{p}})k_{\mathrm{f}},\quad a = 1/F_{\mathrm{p}} \tag{3}$$

For dilute gas mixtures such as the air and water vapor at near atmospheric condition, the relation between the heat and mass transfer can be expressed simply in terms of the Lewis number [16]. Since the Lewis number in the mixture of air and water vapor is close to 1 in general, the following relation can be applied [16].

$$Le_{\mathrm{eff}} = \frac{k_{\mathrm{a,eff}}}{c_{\mathrm{p}}\gamma_{\mathrm{eff}}} \approx 1 \tag{4}$$

$$\frac{h_{\mathrm{i}}}{h_{\mathrm{D}}c_{\mathrm{p}}} = (Le_{\mathrm{eff}})^{2/3} \approx 1 \tag{5}$$

The enthalpy of humid air consists of the sensible heat of both the air and the water vapor and the latent heat of the water vapor. However, since the sensible heat of the water vapor is negligibly small compared with the sensible heat of the air or the latent heat of the water vapor in general, the enthalpy of the humid air can be expressed as [16]

$$i_{\mathrm{a}} = c_{\mathrm{p}}T_{\mathrm{a,db}} + \omega_{\mathrm{a}}i_{\mathrm{fg}} \tag{6}$$

To simplify the analysis, it is assumed that the enthalpy of the air is a linear function of the wet bulb temperature. This assumption implies that the saturation vapor pressure is assumed linearly dependent on the temperature [6]. With this assumption, the enthalpy of the air can be expressed as

$$i_{\mathrm{a}} = c_{\mathrm{wb}}T_{\mathrm{a,wb}} + \mathrm{const} \tag{7}$$

where

$$c_{\mathrm{wb}} = c_{\mathrm{p}} + g_{\mathrm{sat}}i_{\mathrm{fg}} \tag{8}$$

In the above equation, g_{sat} is the gradient of the saturation line in the psychrometric chart. In a real situation, g_{sat} is not constant but varies with the temperature. In this study, g_{sat} is assumed to be a constant holding an average value in the temperature range of concern. Maclaine-Cross and Banks [6] applied this assumption to the analysis of a cooling tower and showed that the error due to the assumption is less than 1.5% in the temperature range of 10–40 °C.

Now, using Eqs. (5) and (6), the energy equations can be transformed into enthalpy equations, and, subsequently by using Eq. (7), the resulting enthalpy equations can be expressed in terms of the wet bulb temperature as follows:

$$k_{\mathrm{a,eff}}\zeta\frac{\partial^2 T_{\mathrm{a,wb}}}{\partial y^2} + h_{\mathrm{i}}a\zeta(T_{\mathrm{f}} - T_{\mathrm{a,wb}}) = \rho U c_{\mathrm{wb}}\frac{\partial T_{\mathrm{a,wb}}}{\partial x} \tag{9}$$

$$k_{\mathrm{f,eff}}\frac{\partial^2 T_{\mathrm{f}}}{\partial y^2} - h_{\mathrm{i}}a\zeta(T_{\mathrm{f}} - T_{\mathrm{a,wb}}) = 0 \tag{10}$$

where

$$\zeta = \frac{c_{\mathrm{wb}}}{c_{\mathrm{p}}} \tag{11}$$

The parameter, ζ, is a factor related to the ratio between the latent heat transfer and the sensible heat transfer. This parameter being one implies the contribution of the evaporative cooling is negligible and the corresponding cooling characteristics approach those of common sensible heat exchangers.

Meanwhile, the mass diffusion equation can be presented as the equation of the humidity ratio considering the air–water vapor mixture being a dilute gas [17].

$$\frac{k_{\mathrm{a,eff}}}{c_{\mathrm{p}}}\frac{\partial^2 \omega_{\mathrm{a}}}{\partial y^2} - h_{\mathrm{D}}a(\omega_{\mathrm{a}} - \omega_{\mathrm{f}}) = \rho U\frac{\partial \omega_{\mathrm{a}}}{\partial x} \tag{12}$$

With the aid of Eq. (12), the equation for the dry bulb temperature can be obtained by subtracting the latent heat terms from the energy equation of the air, Eq. (1).

Now, the boundary conditions are

$$T_{\mathrm{f}}|_{y=H} = T_{\mathrm{a,wb}}\big|_{y=H} = T_{\mathrm{a,db}}\big|_{y=H} = T_{\mathrm{wall}},\quad \omega_{\mathrm{a}}|_{y=H} = \omega_{\mathrm{wall}} \tag{13}$$

$$\left.\frac{\partial T_{\mathrm{f}}}{\partial y}\right|_{y=0} = \left.\frac{\partial T_{\mathrm{a,wb}}}{\partial y}\right|_{y=0} = \left.\frac{\partial T_{\mathrm{a,db}}}{\partial y}\right|_{y=0} = \left.\frac{\partial \omega_{\mathrm{a}}}{\partial y}\right|_{y=0} = 0 \tag{14}$$

Since the wall temperature is not known in advance and should be obtained as a part of the solution, one more equation is required to complete the wall boundary condition. It can be obtained from the energy balance at the channel wall as

$$q_{\mathrm{wall}} = k_{\mathrm{f,eff}}\left.\frac{\partial T_{\mathrm{f}}}{\partial y}\right|_{y=H} + k_{\mathrm{a,eff}}\left.\frac{\partial T_{\mathrm{a,db}}}{\partial y}\right|_{y=H} + \gamma_{\mathrm{eff}}\left.\frac{\partial \omega_{\mathrm{a}}}{\partial y}\right|_{y=H}\cdot i_{\mathrm{fg}} \tag{15}$$

This equation describes the heat transfer at the channel wall as displayed in Fig. 2. Applying the assumption of the Lewis number being unity again, the last two terms can be expressed as a single term of the wet bulb temperature. This results in

$$q_{\mathrm{wall}} = k_{\mathrm{f,eff}}\left.\frac{\partial T_{\mathrm{f}}}{\partial y}\right|_{y=H} + k_{\mathrm{a,eff}}\zeta\left.\frac{\partial T_{\mathrm{a,wb}}}{\partial y}\right|_{y=H} \tag{16}$$

3. Nondimensionalization and exact solutions

3.1. Nondimensionalization

The governing equation can be rendered dimensionless using the following nondimensional variables:

$$\theta = \frac{k_{f,eff}(T - T_{wall})/H}{q_{wall}},$$
$$\Omega = \frac{k_{f,eff}(\omega - \omega_{wall})i_{fg}/(Hc_p)}{q_{wall}}, \quad \eta = \frac{y}{H}. \tag{17}$$

Adding Eqs. (9) and (10) and integrating it over the channel cross section with the aid of boundary conditions, Eqs. (14) and (16), the integrated energy balance is obtained as

$$\rho c_{wb}\left\langle U\frac{\partial T_{a,wb}}{\partial x}\right\rangle = \rho\langle U\rangle c_{wb}\frac{\partial T_{a,wb}}{\partial x} = \frac{q_{wall}}{H} \tag{18}$$

In arriving at the above equation, it is assumed that the flow and thermal fields are fully developed. Equation (18) implies that the wet bulb temperature has a constant gradient along the flow direction under the fully developed condition. By referring to Eqs. (9), (10) and (13), it can be found that the fin and the wall temperature have the same temperature gradient as that of the wet bulb temperature. The dry bulb temperature is also expected to have the same temperature gradient. Accordingly, when the flow and thermal fields are fully developed, all of the wet bulb, the dry bulb, the fin and the wall temperatures have the same temperature gradient along the flow direction such that

$$\frac{\partial T_{a,wb}}{\partial x} = \frac{\partial T_{a,db}}{\partial x} = \frac{\partial T_f}{\partial x} = \frac{\partial T_{wall}}{\partial x} = \frac{q_{wall}}{\rho\langle U\rangle Hc_{wb}}. \tag{19}$$

In practical situations, the fin pitch is much shorter than the fin length. In such cases, it is known that the hydraulic boundary layer is confined to a narrow region near the wall [14,18] and, hence, the fluid velocity is nearly uniform in most of the region inside the channel. Considering this, it is assumed that the flow has a uniform distribution in the channel. Using Eq. (18) and dimensionless variables shown in Eq. (17) with the assumption of uniform flow, the governing equations can be nondimensionalized as

$$\kappa\zeta\frac{\partial^2\theta_{a,wb}}{\partial\eta^2} + Bi\zeta(\theta_f - \theta_{a,wb}) = 1 \tag{20}$$

$$\frac{\partial^2\theta_f}{\partial\eta^2} - Bi\zeta(\theta_f - \theta_{a,wb}) = 0 \tag{21}$$

$$\kappa\frac{\partial^2\theta_{a,db}}{\partial\eta^2} + Bi(\theta_f - \theta_{a,db}) = \frac{1}{\zeta} \tag{22}$$

$$\kappa\frac{\partial^2\Omega_a}{\partial\eta^2} + Bi(\Omega_f - \Omega_a) = 1 - \frac{1}{\zeta} \tag{23}$$

where the parameters, Bi and κ, are defined as

$$Bi = \frac{h_i aH^2}{k_{f,eff}}, \quad \kappa = \frac{k_{a,eff}}{k_{f,eff}}. \tag{24}$$

These two nondimensional parameters will be referred to as the fin parameters. They are determined by the fin material, the fin geometrical shape, the dimensions, and the flow velocity. The parameter Bi is an equivalent Biot number representing the ratio of the thermal conductance associated with the sensible heat exchange between the fin and the air to the conductive conductance through the fin. The parameter κ represents the ratio of the effective thermal conductivities between the air and the fin.

3.2. Exact solutions

The governing equations, Eqs. (20) and (21), and the relevant boundary conditions are very similar to those concerned with the sensible heat transfer in porous media. Referring to the work of Lee and Vafai [19], the corresponding solutions to the evaporative cooling can be obtained as

$$\theta_{a,wb} = \frac{1}{1+\kappa\zeta}\left[\frac{1}{2}(\eta^2 - 1) - \frac{1}{Bi\zeta(1+\kappa\zeta)} \times \left\{1 - \frac{\cosh(\lambda\eta)}{\cosh(\lambda)}\right\}\right] \tag{25}$$

$$\theta_f = \frac{1}{1+\kappa\zeta}\left[\frac{1}{2}(\eta^2 - 1) + \frac{\kappa}{Bi(1+\kappa\zeta)} \times \left\{1 - \frac{\cosh(\lambda\eta)}{\cosh(\lambda)}\right\}\right] \tag{26}$$

where

$$\lambda = \sqrt{Bi(1+\kappa\zeta)/\kappa} \tag{27}$$

It is found that Eq. (22) multiplied by ζ leads exactly to Eq. (20). Therefore, the distribution of the dry bulb temperature should be the same as that of the wet bulb temperature, such that

$$\theta_{a,db} = \theta_{a,wb}. \tag{28}$$

This fact implies that the air stream comes to be fully saturated with the water vapor everywhere in the channel once the flow is thermally fully developed.

The distribution of the water vapor content can be obtained from Eq. (23) and relevant boundary conditions. This can be also obtained more easily by using the thermodynamic relation between the wet bulb temperature, the dry bulb temperatures, and the humidity ratio. Based on the simplified equations, Eqs. (6) and (7) considering the dry bulb and wet bulb temperatures the same, the expression for the humidity ratio is obtained as follows:

$$\Omega_a = (\zeta - 1)\theta_{a,wb}. \tag{29}$$

4. Results and discussions

4.1. Temperature profiles

The temperature distributions of the air and the fin in the evaporative cooler are shown in Fig. 3 for two different values of the Biot number, 0.5 and 10. The effective conductivity ratio, κ, is given a small value, 0.01. For typical plate fin heat exchangers, the parameters, Bi and κ, range from 0.1 to 10 and from 10^{-4} to 10^{-1}, respectively. This will be discussed more in detail in a later section. The temperature distributions are for the case where $\zeta = 4$ which corresponds to the condition with the temperature around 25 °C. For the purpose of comparison, the temperature distributions in a sensible cooler [19] are also shown in the figures. They can be obtained from Eqs. (25) and (26) by setting ζ to one. The subscripts, E and S, in the figure indicate the evaporative cooler and the sensible cooler, respectively. Note that the subscripts to distinguish between the wet bulb and the dry bulb temperatures in the evaporative cooler are omitted in Fig. 3 because there is no difference between the two temperatures under fully developed condition.

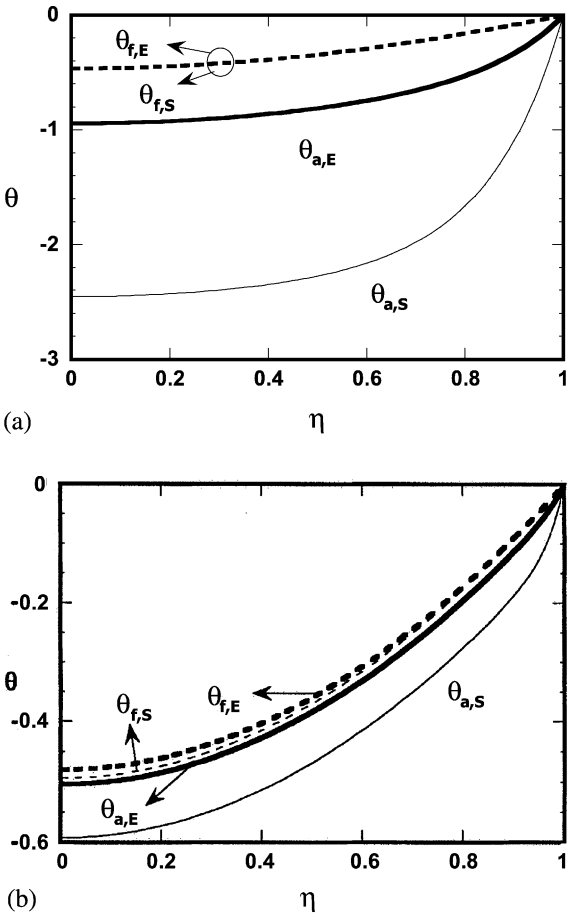

Fig. 3. Comparison of the temperature profiles ($\zeta = 4$): (a) $Bi = 0.5$ and $\kappa = 0.01$; (b) $Bi = 10$ and $\kappa = 0.01$.

It is seen that the temperature difference between the channel wall and the air in the evaporative cooler is smaller than that in the sensible cooler though the degree depends on the Biot number. The decrease in the temperature difference is due to the fact that the cooling effect in the evaporative cooler is caused by the latent heat transfer as well as by the sensible heat transfer. Accordingly, a smaller temperature difference is required for the same heat rate being dissipated in the evaporative cooler than in the sensible cooler, which implies that the cooling performance is enhanced due to the evaporative cooling. Meanwhile, the fact that the degree of decrease in the temperature difference depends on the Biot number indicates the cooling enhancement depends on that parameter.

4.2. Cooling enhancement

The heat transfer coefficient and the Nusselt number in the evaporative cooler are defined as follows:

$$h_w = \frac{q_{wall}}{T_{wall} - \langle T_a \rangle} \tag{30}$$

$$Nu_E = \frac{h_w 4H}{k_{a,eff}} = \frac{4}{\kappa(-\langle \theta_a \rangle)} \tag{31}$$

Using Eqs. (25) and (31), the Nusselt number is obtained as

$$Nu_E = 12\frac{1+\kappa\zeta}{\kappa}\frac{1}{1+\frac{3}{Bi\zeta(1+\kappa\zeta)}\left\{1-\frac{1}{\lambda}\tanh(\lambda)\right\}} \tag{32}$$

The ratio of the Nusselt numbers between the evaporative and the sensible coolers is depicted in Fig. 4 for the case where $\zeta = 4$. The Nusselt number in the sensible cooler can be readily obtained also from Eq. (32) by substituting one for ζ. It is found that the ratio of the Nusselt numbers is nearly 4 in most of the range of the parameters covered in this figure. This implies that the cooling performance increases four times larger by applying the evaporative cooling. This is because the thermal conductance between the channel wall and the air is increased four times larger due to the addition of the latent heat transfer to the basic sensible heat transfer in an air-cooled heat exchanger.

Meanwhile the Nusselt number ratio decreases as κ decreases below one and Bi increases beyond one. This finding is important from a practical point of view, since the typical range of the parameters in finned heat exchangers belongs to this region as displayed in Fig. 4. In other words, the cooling enhancement when applying the evaporative cooling to an air-cooled heat exchanger depends greatly on the fin parameters, κ and Bi.

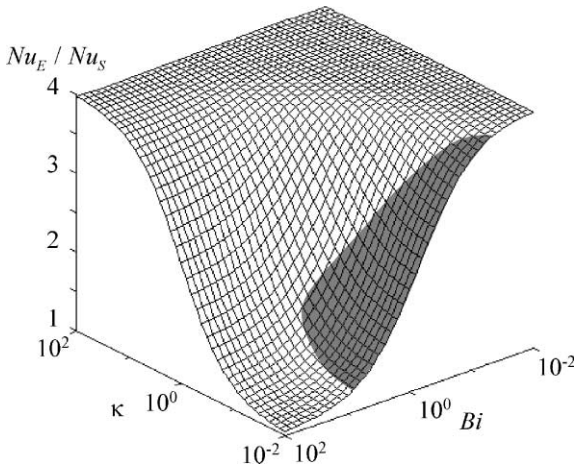

Fig. 4. Nusselt number ratio between the evaporative and the sensible coolers ($\zeta = 4$).

The asymptotic behavior of the cooling enhancement in the typical range of the parameters can be obtained from Eq. (32), by using the following asymptotic relation in this range:

$$\frac{1}{\lambda}\tanh(\lambda) \approx 1/\lambda \quad \text{as} \quad \lambda \to \infty, \tag{33}$$

as follows:

$$\frac{Nu_E}{Nu_S} \approx \frac{1 + 3/Bi}{1 + 3/(Bi\zeta)} \tag{34}$$

This equation reveals that the ratio converges to a maximum value ζ when Bi becomes less than one, while it decreases and the enhancement vanishes as Bi becomes greater than one.

4.3. Influences of the fin parameters on the cooling enhancement

To show the reason why the cooling enhancement depends on the fin parameters, a typical geometric configuration of the louvered fin heat exchanger is considered as a case. The fin thickness and the fin pitch are taken as the main dimensional variables, and the influences of the subsequent changes in the fin parameters, κ and Bi, are investigated. In this instance, the fin height is 10 mm; the fin length in the flow direction is 30 mm; the louver angle is 30°; and the air velocity is 3 m/s. The geometric dimensions of the fin configuration including those mentioned above are arranged in Table 1. The relevant definition of the geometric parameters is shown in Fig. 1.

Once the fin geometric dimensions are determined, the effective conductivities of the fin and the air, and the specific surface area of the fin can be evaluated from Eq. (3). For the interstitial heat transfer coefficient, h_i, the following j factor correlation for corrugated louver fin with rectangular channel [20] can be referred to:

$$j = Re_{Lp}^{-0.49}\left(\frac{\Theta_L}{90}\right)^{0.27}\left(\frac{F_p}{L_p}\right)^{-0.14}\left(\frac{F_l}{L_p}\right)^{-0.29}\left(\frac{T_d}{L_p}\right)^{-0.23} \times \left(\frac{L_l}{L_p}\right)^{0.68}\left(\frac{T_p}{L_p}\right)^{-0.28}\left(\frac{F_t}{L_p}\right)^{-0.05} \tag{35}$$

The interstitial heat transfer coefficient, h_i, is calculated from the definition of j factor as follows:

$$j = St \cdot Pr^{2/3} = \frac{h_i}{v\rho c_p} Pr^{2/3} \tag{36}$$

With the values of $k_{f,eff}$, $k_{a,eff}$, a and h_i evaluated from above, the two important fin parameters, Bi and κ, can now be calculated using Eq. (24).

Fig. 5 shows the variations of the two parameters, Bi and κ, in accordance with the changes in the fin pitch and the fin thickness. The fin thickness is varied from 0.01 to 0.3 mm for two different values of the fin pitch, 1 and 3 mm. This range of the values is believed to cover most of the application in the louvered fin heat exchangers [20,21]. It can be seen from Fig. 5 that, in this typical range of the fin dimensions, the Biot number and κ vary from 0.1 to 10 and from 10^{-4} to 10^{-1}, respectively. The values of both the Biot number and κ decrease as the fin thickness increases. This is due to the increase in the effective conductivity of the fin with an

Table 1
Geometric dimensions of a louvered fin exchanger

Channel width	10 mm	Fin length	10 mm
Louver angle	30°	Louver pitch	1 mm
Tube depth	30 mm	Tube pitch	12 mm
Louver length	8 mm	Fin pitch, fin thickness	Variable

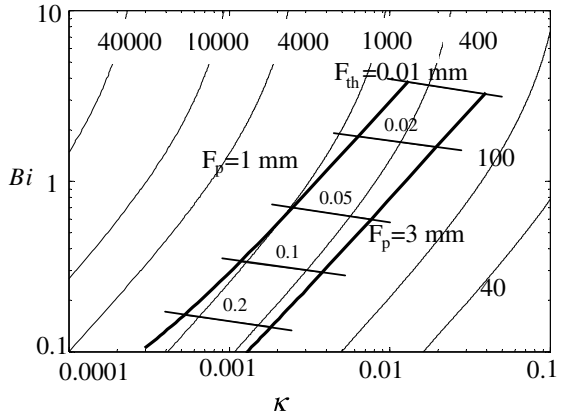

Fig. 5. Nusselt number variation with changes in fin parameters in sensible coolers.

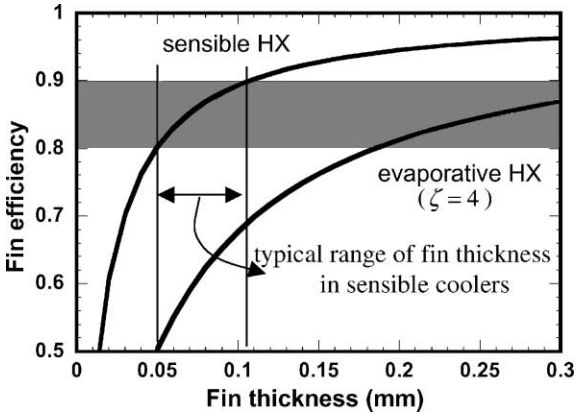

Fig. 6. Fin efficiency with respect to the fin thickness.

increase in the fin thickness as can be seen from the definitions of the parameters, Eqs. (3) and (24).

The background of the figure shows the contours of the Nusselt number in sensible coolers without water evaporation. As the fin thickness increases, the Nusselt number increases and eventually converges to a constant value.

The effect of the fin thickness can be seen more clearly in Fig. 6 which shows the variation of the fin efficiency with changes in the fin thickness when $F_p = 1$ mm. The fin efficiency is defined as

$$\eta_f \equiv \frac{q_f}{q_{max}} = \frac{h_i a(\langle T_f\rangle - \langle T_a\rangle)}{h_i a(T_{wall} - \langle T_a\rangle)} = \frac{\langle\theta_a\rangle - \langle\theta_f\rangle}{\langle\theta_a\rangle} = 1 - \frac{\langle\theta_f\rangle}{\langle\theta_a\rangle} \quad (37)$$

In Fig. 6, the fin efficiency in the sensible cooler is depicted together with that in the evaporative cooler when $\zeta = 4$. When the fin is thicker than 0.1 mm, the fin efficiency in the sensible cooler is relatively large and increases slowly with an increase in the fin thickness, while it decreases rapidly for a fin thinner than 0.1 mm. Obviously, this is the reason for the Nusselt number variation in the sensible cooler with respect to the fin thickness variation shown in Fig. 5.

The fin efficiency is shown to drop considerably when evaporative cooling is applied to the sensible cooler. This is due to the increase in the thermal conductance between the fin and the air resulting from the latent heat transfer by the water evaporation from the thin water film on the fin surface. The increase in the thermal conductance between the fin and the air causes a relative decrease in the conductive conductance through the fin, which results in the decrease in the fin efficiency. When the fin efficiency decreases, the cooling enhancement due to the evaporative cooling also decreases compared with what would be achieved without the decrease in the fin efficiency.

It is seen that the decrease in the fin efficiency is largely dependent on the fin thickness. The decrease in the fin efficiency is more severe for a thinner fin. Consequently, the degree of cooling enhancement decreases as the fin gets thinner. This is the reason why the cooling enhancement by evaporative cooling depends on the fin parameters in Fig. 4.

If the fin efficiency is designed between 0.8 and 0.9, the fin thickness in a sensible cooler can be determined from Fig. 6 between 0.05 and 0.1 mm. The cooling enhancement by applying the water evaporation to this sensible cooler would not be sufficiently large compared with the theoretical maximum due to the decrease in the fin efficiency as shown in Fig. 6. If the thickness is increased larger for higher fin efficiency, the cooling enhancement can be increased approaching the theoretical maximum value.

5. Conclusions

A theoretical analysis on the heat transfer enhancement with the application of evaporative cooling to an air-cooled finned heat exchanger is presented in this work. A 2-D model on the heat and mass transfer process in a finned channel is developed adopting a porous medium approach. Based on this model, the characteristics of the heat and mass transfer are investigated in a plate-fin heat exchanger with the interstitial surface fully covered by thin water film. The theoretical solutions to the temperature and the moisture distributions are obtained and the Nusselt number is evaluated. When the interstitial surface is covered with thin water film, the temperature difference between the channel wall and the air becomes smaller due to the water evaporation from the fin surface and subsequent latent heat dissipation. Consequently, the cooling effect improves considerably compared with that in the sensible cooler without water evaporation. The maximum cooling enhancement is by a factor of ζ which is associated with the ratio between the latent heat of the water evaporation and the sensible heat of the air.

In a typical finned heat exchanger incorporating evaporative cooling, the cooling enhancement is usually less than the maximum value, and depends on the ratio of the thermal conductance between the fin and the air to the conductive conductance through the fin. From the practical point of view, this ratio is mostly dependent on the fin thickness and thus the cooling enchancement also becomes dependent on this parameter. When the fin is not sufficiently thick, the cooling enhancement by the evaporative cooling decreases since the fin efficiency drops due to the water evaporation from the fin surface. Therefore, the fin thickness in the evaporative cooler should be increased compared with that in the sensible cooler to take full advantage of the evaporative cooling.

Acknowledgement

This work was supported by the Brain Korea 21 project.

References

[1] W.-J. Yang, D.W. Clark, Spray cooling of air-cooled compact heat exchangers, Int. J. Heat Mass Transfer 18 (1975) 311–317.
[2] H. Perez-Blanco, W.A. Bird, Study of heat and mass transfer in a vertical-tube evaporative cooler, ASME, J. Heat Transfer 106 (1984) 210–215.
[3] K.M. Graham, S. Ramadhyani, Experimental and theoretical studies of mist jet impingement cooling, ASME, J. Heat Transfer 118 (1996) 343–349.
[4] S. Chuntranuluck, C.M. Wells, A.C. Cleland, Prediction of chilling times of foods in situations where evaporative cooling is significant—Part 2. Experimental testing, J. Food Eng. 37 (1998) 127–141.
[5] M. Sweetland, J.H. Lienhard, Evaporative cooling of continuously drawn glass fibers by water sprays, Int. J. Heat Mass Transfer 43 (2000) 777–790.
[6] I.L. Maclaine-Cross, P.J. Banks, A general theory of wet surface heat exchangers and its application to regenerative evaporative cooling, ASME, J. Heat Transfer 103 (1981) 579–585.
[7] C.F. Kettleborough, C.S. Hsieh, The thermal performance of the wet surface plastic plate heat exchanger used as an indirect evaporative cooler, ASME, J. Heat Transfer 105 (1983) 366–373.
[8] S.T. Hsu, Z. Lavan, W.M. Worek, Optimization of wet-surface heat exchangers, Energy 14 (1989) 757–770.
[9] P.L. Chen, H.M. Qin, Y.J. Huang, H.F. Wu, A heat and mass transfer model for thermal and hydraulic calculations of indirect evaporative cooler performance, ASHRAE Trans. (1991) 852–865.
[10] N.J. Stoitchkov, G.I. Dimitrov, Effectiveness of crossflow plate heat exchanger for indirect evaporative cooling, Int. J. Refrig. 21 (1998) 463–471.
[11] Y.L. Tsay, Analysis of heat and mass transfer in a countercurrent-flow wet surface heat exchanger, Int. J. Heat Fluid Flow 15 (1994) 149–156.
[12] W.-M. Yan, Effect of film vaporization on turbulent mixed convection heat and mass transfer in a vertical channel, Int. J. Heat Mass Transfer 38 (1995) 713–722.
[13] W.-M. Yan, Evaporative cooling of liquid film in turbulent mixed convective channel flows, Int. J. Heat Mass Transfer 41 (1998) 3719–3729.
[14] S.J. Kim, D. Kim, Forced convection in microstructures for electronic equipment cooling, ASME J. Heat Transfer 121 (1999) 639–645.
[15] S.J. Kim, D. Kim, D.-Y. Lee, On the local thermal equilibrium in microchannel heat sinks, Int. J. Heat Mass Transfer 43 (2000) 1735–1748.
[16] ASHRAE, ASHRAE Handbook-Fundamentals. American Society of Heating, Refrigerating and Air-Conditioning Engineers, Inc., 1997 (Chapters 5–6).
[17] W.M. Kays, M.E. Crawford, Convective Heat and Mass Transfer, third ed., McGraw-Hill, Inc., New York, 1993 (Chapter 4).
[18] D.-Y. Lee, J.S. Jin, B.H. Kang, Momentum boundary layer and its influence on the convective heat transfer in porous media, Int. J. Heat Mass Transfer 45 (2002) 229–233.
[19] D.-Y. Lee, K. Vafai, Analytical characterization and conceptual assessment of solid and fluid temperature differentials in porous media, Int. J. Heat Mass Transfer 42 (1999) 423–435.
[20] Y.-J. Chang, C.-C. Wang, A generalized heat transfer correlation for louver fin geometry, Int. J. Heat Mass Transfer 40 (1997) 533–544.
[21] W.M. Kays, A.L. London, Compact Heat Exchangers, third ed., McGraw-Hill, Inc., New York, 1984.